A 2000-Year Tree Ring Record of Annual Temperatures in the Sierra Nevada Mountains

Louis A. Scuderi

Science, New Series, Vol. 259, No. 5100 (Mar. 5, 1993), 1433-1436.

tion, local minimization, Fourier synthesis, and peak picking. By observing the resulting values of $R(S)$ over the set of trials that have been processed, we are able to determine whether or not a solution has been obtained.

Based on experimentation with respect to the 28-atom, 84-atom, and 127-atom structures, we conjecture that the number of cycles of Shake-and-Bake necessary to determine the structures under consideration is of the order of 1.5 times the number of atoms in the structure. Therefore, we chose to perform the algorithm for 150 cycles on both of the previously unknown ~100-atom structures.

Experimentation on the 84-atom and 127-atom structures indicates that a cost-effective ratio for phases to atoms is approximately 10 to 1, while a cost-effective ratio for triples to phases is approximately 20 to 1, and the incorporation of negative quartets (that is, $B < 0$) may be unnecessary.

The experimentation described in this report has been performed predominantly on a Connection Machine CM-5 at Thinking Machines Corporation. Pertinent details of the experiments are given in Table 1. For both previously unknown structures, it was assumed that there were 104 atoms, although we subsequently found this not to be the case. Nevertheless, we used 104 atoms in the procedure. Further, based on the 10:1 phase to atom ratio and 20:1 triplet to phase ratio (no quartets), we chose to use 1,000 phases, 20,000 triples, and 0 quartets. Notice that in the case of ternatin(I), a number of reflections were removed from the full data set that corresponded to h indexes of 9 through 11 on the basis that their $F/\sigma(F)$ ratios were abnormally small. We chose to run the algorithm for 150 cycles using the 1.5:1 cycle to atom ratio. Based on available computer time, and desiring a sufficient sample size, we processed 2048 initial, randomly generated starting structures.

The six solutions produced for ternatin(I) had final $R(\Phi)$ values in the [0.45, 0.46] range, whereas the nonsolutions had final $R(\Phi)$ values greater than 0.49. The 19 solutions produced for ternatin(II) had final $R(\Phi)$ values in the [0.41, 0.42] range, whereas the nonsolutions had final $R(\Phi)$ values greater than 0.46. In other words, as mentioned previously, $R(\Phi)$ is diagnostic in terms of detecting solutions. A visual representation of the convergence of a solution versus a nonsolution for ternatin(I) with respect to $R(\Phi)$ is shown in Fig. 3. In fact, based solely on the final $R(\Phi)$ values, we were able to determine that after 64 trials of ternatin(I) a single solution was at hand, and that after 64 trials of ternatin(II) there were two solutions. Each initial 64-trial experiment was performed in ~70 CPU min on a 64-node Connection Machine CM-5. It was only later that we decided to run both structures for 2048 trials for statistical purposes. The percentage of success was significantly higher for ternatin(II) than for ternatin(I). This difference may be due to the fact that there was a threefold higher percentage of aberrant triples with high A values for ternatin(I) as compared to ternatin(II), which more nearly matched the expected rate of failure predicted by the A-values.

REFERENCES AND NOTES

1. G. DeTitta *et al.*, in *Proceedings of the Sixth Distributed Memory Computing Conference* (IEEE Computer Society, New York, 1991), pp. 587–594.
2. C. M. Weeks, G. T. DeTitta, R. Miller, H. A. Hauptman, *Acta Crystallogr. D* **49**, 179 (1993).
3. N. Bashir *et al.*, in *Proceedings of the Fifth Distributed Memory Computing Conference* (IEEE Computer Society, New York, 1990), pp. 513–521.
4. H. A. Hauptman, *Abstr. Am. Crystallogr. Assoc.* **16**, 53 (R4) (1988).
5. H. A. Hauptman, *Crystallographic Computing 5: From Chemistry to Biology*, D. Moras, A. D. Podjarny, J. C. Thierry, Eds. (Oxford Univ. Press, New York, 1991), pp. 324–332.
6. C. Weeks, W. Duax, M. Wolff, *Acta Crystallogr. B* **32**, 261 (1976).
7. V. Z. Pletnev, N. Galitsky, G. Smith, C. Weeks, W. Duax, *Biopolymers* **19**, 1517 (1980).
8. V. Z. Pletnev, V. T. Ivanov, D. A. Langs, P. Strong, W. L. Duax, *ibid.* **32**, 819 (1992).
9. Crystals were grown by slow evaporation from dioxane. Data were recorded in 1982 at room temperature with CuKα radiation on a Syntex P1 diffractometer to a resolution of 0.94 Å in which a 96-step $\theta - 2\theta$ scanning procedure was used. Crystal data: $2(C_{37}H_{67}N_7O_8)\cdot C_4H_8O_2$, orthorhombic $P2_12_12_1$, a = 11.563(1), b = 21.863(2), c = 36.330(4) Å (numbers in parentheses are errors in the last digit), and Z = 4.
10. Crystals were grown by slow evaporation from 95% ethanol. Data were recorded in 1990 at 153 K with CuKα radiation on a Nonius CAD4 diffractometer to a resolution of 0.97 Å in which a similar $\theta - 2\theta$ step scan procedure was used. Crystal data: $2(C_{37}H_{67}N_7O_8)\cdot H_2O$, orthorhombic $P2_12_12_1$, a = 14.067(2), b = 16.695(1), c = 36.824(4) Å, and Z = 4.
11. J.-X. Yao, *Acta Crystallogr. A* **37**, 642 (1981).
12. M. G. Rossmann, Ed., *The Molecular Replacement Method* (Gordon and Breach, New York, 1972).
13. R. Miller *et al.*, unpublished results.
14. T. Debaerdemaeker, C. Tate, M. M. Woolfson, *Acta Crystallogr. A* **44**, 353 (1988).
15. G. M. Sheldrick, *ibid.* **46**, 467 (1990).
16. M. Shiono and M. M. Woolfson, *ibid.* **48**, 451 (1992).
17. E. H. L. Aarts and P. J. M. van Laarhoven, *Simulated Annealing: Theory and Applications* (Reidel, New York, 1988).
18. D. E. Holland, *Genetic Algorithms in Search, Optimization, and Machine Learning* (Addison-Wesley, Reading, MA, 1989).
19. C.-S. Chang *et al.*, *Int. J. Supercomput. Appl.*, in press.

20. Supported by NIH grants GM-46733, GM-32812, and DK-19856 (in part), NSF grant IRI-9108288 and the Harker grant. We thank N. Galitsky for x-ray diffraction data collection; C.-S. Chang, A. Khalak, C.-W. Lee, and P. Thuman, who performed some of the computational experiments described in this report; and the Thinking Machines Corporation for allowing us to use their CM-5 machines.

2 October 1992; accepted 5 January 1993

A 2000-Year Tree Ring Record of Annual Temperatures in the Sierra Nevada Mountains

Louis A. Scuderi

Tree ring data have been used to reconstruct the mean late-season (June through January) temperature at a timberline site in the Sierra Nevada, California, for each of the past 2000 years. Long-term trends in the temperature reconstruction are indicative of a 125-year periodicity that may be linked to solar activity as reflected in radiocarbon and auroral records. The results indicate that both the warm intervals during the Medieval Warm Epoch (~A.D. 800 to 1200) and the cold intervals during the Little Ice Age (~A.D. 1200 to 1900) are closely associated with the 125-year period. Significant changes in the phase of the 125-year temperature variation occur at the onset and termination of the most recent radiocarbon triplet and may indicate chaotic solar behavior.

Knowledge of temperature variability on century to millennium time scales is important to understanding the magnitude of natural climate forcings and is critical to differentiating between these effects and those of recent anthropogenic forcings. There are few well-calibrated long temperature series in existence that can be used to reconstruct this variability. Analysis of living and remnant wood of foxtail pine (*Pinus balfouriana*) from the southern Sierra Nevada has yielded an absolutely dated series of ring widths that extends back to 1050 B.C. (*1*) and an absolute and radiocarbon-dated chronology of timberline position to ~4400 B.C. (*2*). At the upper timberline, the growth of this tree is closely related to seasonal temperature (*3–5*). I used this tree ring record to reconstruct temperature anomalies for a growth season, which is defined as June through January. In this report, I analyze the century-scale variability in this record.

Department of Geography, Boston University, Boston, MA 02215.

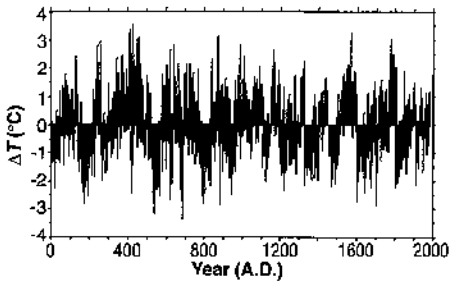

Fig. 1. Reconstructed June through January temperature anomalies for southern Sierra Nevada relative to the A.D. 1 to 1980 mean. The A.D. 1951 to 1970 reference temperature is 0.12°C above the long-term mean.

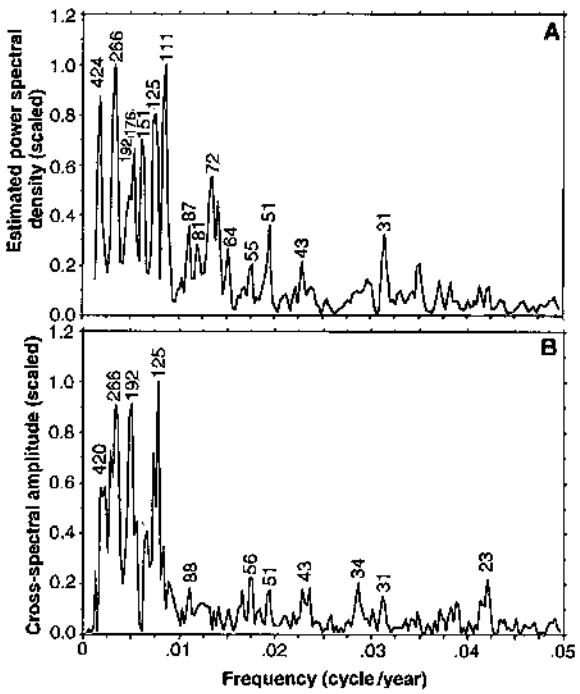

Fig. 2. (**A**) Power spectral density of the Cirque Peak temperature sequence (1050 B.C. to A.D. 1981). Significant century-scale peaks ($P \leq 0.05$) are indicated at ~424, 266, 176, 151, 125, and 111 years. (**B**) Cross-spectral analysis of the Cirque Peak ring width record and $\Delta Q/Q_t$ (1050 B.C. to A.D. 1870). Significant century-scale peaks ($P \leq 0.05$) are indicated at ~420, 266, 192, and 125 years (confidence intervals $2\sigma = \pm 15$, 12, 11, and 7 years, respectively). All are harmonics of a 2120-year fundamental Hallstattzeit variation (*19*, *20*). The ~192-year period may be a poorly resolved expression of the significant ~200-year period found in the radiocarbon record.

I used a standardization approach in which the data are fit with an equation of exponential decay, G_t, of the form

$$G_t = a\,e^{-bt} + k \qquad (1)$$

for year t, where a, b, and k are coefficients of the nonlinear regression function that is fit to the data (*6*). This is in contrast to the low-order polynomial detrending method (*7*) that was used in earlier analyses of this chronology (*1*, *8*). This standardization approach has been found to be most appropriate for open canopy stands (*6*), such as at Cirque Peak, where disturbance and competition are minimal. I corrected several of the component series from the earlier work (*1*, *8*) to reflect a cross-dating anomaly between A.D. 1300 and 1350 (*9*).

Following standard procedures (*3*, *5*), I determined the optimal season for reconstruction with a combination of temperature response function analysis (*3*, *10*) and regression analysis. Response function analysis (*1*) indicates that meteorologic conditions of the prior season, especially the temperatures in late fall and early winter, affect tree growth significantly at the site. Results of a forest-ecosystem model (FOREST-BGC) (*11*) support this notion and indicate that spring precipitation likely plays only a minor role in limiting growth at this site. Model results indicate that growth is enhanced by warm summer, fall, and winter temperatures.

Table 1. Calibration of the reconstruction equation. Summary of regression results for the individual 25-year calibrations and of the final regression equation that used the entire 50 years of data. The A.D. 1931 to 1955 reconstruction was verified with the use of the 1956 to 1980 data, while that for 1956 to 1980 was verified with the 1931 to 1955 data. Calibration and verification statistics represent the percent of the variance that is explained by the reconstruction.

	1931 to 1955	1956 to 1980	1931 to 1980
Calibration (%)	65	33	50
Verification (%)	34	64	
Reduction of error	0.10	0.25	
Risk	−0.65	−0.34	
Bias	−0.08	−0.17	
Covariance	0.63	0.76	
Spearman correlation	0.59	0.78	0.69
First difference: sign test			
Correct signs	20	16	37
Incorrect signs	4	8	12
Regression weights			
b_1	4.55	3.227	4.26
b_2	1.18	−0.698	0.14
b_3	1.89	1.140	1.69

Photosynthesis in trees at high latitude (*12*) and high altitude (*3*, *13*) continues into the fall, even though the actual cambial cell division may take place over as little as 4 to 6 weeks during the summer. This results in the production and storage of carbohydrates and other substances that will aid growth in the next year. A warm fall allows this storage to take place, whereas an early or cold fall can prevent bud maturation and full cuticular development of the needles (*4*). Needles with incomplete development are vulnerable to winter desiccation. In a year of good growth, buds form with potential for good growth in the following year. The degree to which this potential is realized is determined by the conditions of the following year (*12*).

Response function and multiple regression analyses (*1*, *8*) suggest that mean temperatures for June through January in earlier years can be usefully reconstructed from tree ring data from the southern Sierra Nevada. Positive coefficients for ring width up to 2 years before the growth year imply that lagged ring width must be included in the regression model. I therefore used a regression equation of the form

$$T_t = b_1\mathrm{INX}_t + b_2\mathrm{INX}_{t+1} + b_3\mathrm{INX}_{t+2} \qquad (2)$$

where T_t is the mean June through January station temperature at Giant Forest–Grant Grove in the southern Sierra Nevada and INX_t is the ring width data in year t.

Having established the potential for the reconstruction of average June through January temperatures and determined the form of the regression equation, I used a cross-calibration and verification exercise to test the general form of the reconstruction equation. The mean June through January temperature series was divided into two 25-year periods: 1931 to 1955 and 1956 to 1980. Then I fit Eq. 2 to one period and applied the derived coefficients to the tree growth data over the other period to give temperature estimates that could be compared with the observed climate data. The process was then repeated with the periods reversed. The results (Table 1) show that 33 to 65% of the independent temperature variance is recovered in the estimated data. For the 1956 to 1980 verification period, the reduction-in-error statistic (RE) was 0.10, whereas for the 1931 to 1955 verification period, RE was 0.25. Values above zero indicate that the reconstruction approach is useful for climate prediction (*3*, *14*, *15*). Having shown the validity of the general regression model, I recalibrated the reconstruction equation using the entire 50 years of climate data.

The reconstructed temperature series, which starts at A.D. 1 (Fig. 1), shows that temperature has varied in a coherent man-

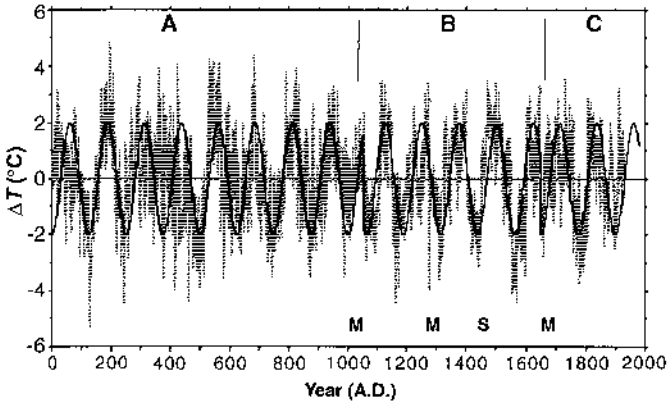

Fig. 3. The 50-year linear trend in the Cirque Peak series (hatched area). The last data point represents the trend from A.D. 193 to 1980. The solid line represents a 125-year period sine wave. Its equation in region A is $2\cos(2\pi t/125 + 0.05\pi)$. Major discontinuities in the phase of the 125-year period are indicated at the onset (~A.D. 1050) and termination (~A.D. 1650) of the most recent triplet set of radiocarbon anomalies (*25*), which is indicated by region B and is described by the equation $2\cos(2\pi t/125 + 0.96\pi)$. Phase remains constant during the triplet, after which, in region C, the graph follows $2\cos(2\pi t/125 + 1.5\pi)$. Events of the Maunder (M) and Spörer (S) types are indicated.

ner with alternating periods of warm and cold over the last 2000 years. The warmest years were A.D. 425 (+3.57°C) and 1569 (+3.25°C), whereas the coldest was A.D. 685 (−3.38°C) (Table 2). The second coldest year, A.D. 536 (−3.13°C), corresponds to the second coldest year (−2.0°C) in the Fennoscandian temperature record (*5*) and may be related to a volcanic eruption that is recorded in the acidity record from the Camp Century, Greenland, ice core and in historical records (*16*). Effects of volcanic eruptions have been shown to influence the high-frequency (<10 years) portion of the Sierra Nevada temperature record (*1*).

The dendroclimatically reconstructed summer temperature record from Fennoscandia (*5*) provides an important reference that can be compared with the record from the southern Sierra Nevada. In general, warming and cooling temperature trends on all time scales are similar to those found in the Fennoscandia (*5*); however, there appears to be a greater degree of coherence between the two records during intervals of cooling. The similarity of the temperature series suggests that the two regions are responding to similar temperature forcings that affect the Northern Hemisphere. However, for the A.D. 1700 to 1900 interval, minor differences exist in the reconstructions: the Fennoscandian series appears to lead that of the southern Sierra Nevada. Comparison of the Sierra Nevada data with a bristlecone pine series from Campito Mountain in the neighboring White Mountains (*13*, *14*, *17*) indicates that these two upper timberline chronologies are in phase over this same interval. During this interval, the temperature variation of the western United States as reconstructed from a grid of arid site conifers (*15*, *18*) has also been shown to be out of phase with that of Europe. Fritts (*15*) has shown that temperatures declined in the western United States in the 1910s and 1920s in contrast to much of the remainder of the world, which experienced warming. This regional cooling may have been associated with large anomalies in air pressure at sea level over the North American Arctic and the North Pacific (*15*).

Analysis of long-term trends indicates that there are periodic variabilities in the Cirque Peak temperature reconstruction. The power spectral density (PSD) (Fig. 2A) of the reconstructed temperature record shows significant spectral lines ($P \leq 0.05$) at periods of ~420, 266, 176, 151, 125, and 111 years. Although periodic variations may appear as the result of a number of processes, the similarity of these spectral lines with those of the radiocarbon record (*19*–*21*) suggests that variability in solar activity may underlie the temperature variability that was recorded in the southern Sierra Nevada. Causal links between solar variability and climate have been suggested (*22*); however, as noted by Stuiver *et al.* (*23*), the correlation between climate and the ^{14}C production rate (Q) is usually weak, but an observable link, although unlikely to be found for most regions, may be observable at selected high-altitude sites. Past work on the spectra of the growth of high-altitude bristlecone pines in the neighboring White Mountains and radiocarbon variations (*24*) appears to support a connection.

The radiocarbon record shows significant power at periods greater than 200 years. A major long period variation in total solar irradiance, namely, the 2120-year Hallstattzeit fundamental and its harmonics, which include the 420-year fundamental (*25*), may be driving climate change (*19*, *20*). The Cirque Peak record (Fig. 2A) reveals a similar pattern of major spectral lines. Many of these periodicities are harmonics of a 2120-year Hallstattzeit fundamental. Cross-spectral analysis between the entire 3050-year Cirque Peak series and the detrended ^{14}C production rate ($\Delta Q/Q_t$) (*26*) (Fig. 2B) reveals the strongest line at ~125 years, which corresponds to a pronounced 127-year peak that is in the last quarter of the radiocarbon record (*25*) and an ~130-year peak in auroral observations (*27*).

The importance of the 125-year period is best illustrated with respect to the 50-year temperature trend at the Cirque Peak site. The trend is in ΔT_{50}, the difference in annual temperatures that are separated by 50 years ($T_{t+50} - T_t$) (Fig. 3). A sine wave of the form

$$\Delta T_{50} = 2.0 \cos\left(\frac{2\pi}{125} t + 0.05\pi\right) \quad (3)$$

that begins at t_0 = A.D. 1 can be fit to this

Table 2. Extreme temperature anomalies for individual years and 20-year means.

Positive		Negative	
Temperature anomaly (°C)	Year or period	Temperature anomaly (°C)	Year or period
	Individual year		
3.57	425	−3.38	685
3.25	1569	−3.13/−3.07/−2.93	536/535/541
3.14	874	−2.87	1703
3.03	1779	−2.85	881
2.96	256	−2.83	176
2.83	986	−2.77	794
2.82	641	−2.72	1604
	20-Year mean		
1.66	1564 to 1583	−1.95	542 to 561
1.45	408 to 427	−1.60	172 to 191
1.42	1786 to 1805	−1.26	1613 to 1632
1.18	1161 to 1180	−1.23	800 to 819
0.97	1439 to 1458	−1.22	1817 to 1836
0.94	1314 to 1333	−1.12	941 to 960

temperature pattern. The fit can be improved significantly by adjusting the phase relation at the onset (~A.D. 1100) and termination (~A.D. 1700) of the most recent clusters of radiocarbon anomalies (triplet episode) (25). This result is similar to that of Stuiver and Braziunas (25), who found that triplet episodes in the production rate ($\Delta Q/Q_t$) of ^{14}C were modeled differently than those of nontriplet intervals. Damon and Jirikowic (20) suggested that during the Hallstattzeit variations, Maunder-type anomalies may be exaggerated, which would lead to more extreme solar variation. Although the amplitude of the 50-year temperature trend during the triplet does not increase, the phase changes significantly at the beginning and end of the triplet. In the temperature reconstruction, the initial change of phase occurs at ~A.D. 1050 and corresponds to the timing of the peak of the first Maunder-type event in the triplet (25). This triplet interval is best fit by

$$\Delta T_{50} = 2.0 \cos\left(\frac{2\pi}{125} t + 0.96\pi\right) \quad (4)$$

This phase relation is terminated between A.D. 1650 and 1680, during the last Maunder-type event in the sequence. The phase change at the end of the triplet amounts to an additional 0.54π (~35 years). Feynman and Gabriel (28) found a similar change in phase in the 88-year Gleissberg cycle as the sun exited the Maunder minimum. They suggested that the sun exhibits periods of suppressed activity during which the phase of periodic variations is not conserved and that this behavior conforms to a chaotic solar dynamo. The appearance of phase changes in the 125-year period at the beginning and the end of the most recent set of major radiocarbon anomalies, as well as the maintenance of phase relations from ~A.D. 1050 to the termination of the prior triplet type event (~200 B.C.), supports this view and, in addition, suggests that the periodicities in the temperature reconstruction from the southern Sierra Nevada were solar-induced. The 600-year duration of anomalous phase (~A.D. 1050 to 1650) also corresponds to the average length of the Hallstattzeit variation (19, 20), whereas spectral peaks in the tree ring temperature reconstruction correspond to harmonics of the 2120-year recurrence interval between such events (19, 20). This comparison indicates that solar variability and climate may be closely related. In light of the findings (25) of significant power between 123 and 143 years in six of ten climate records (tree rings and glacier fluctuations) (29), it is likely that this solar-climate relation is at least marginally detectable globally.

REFERENCES AND NOTES

1. L. A. Scuderi, *Quat. Res. (NY)* **27**, 220 (1987); *ibid.* **34**, 66 (1990).
2. ———, *Nature* **325**, 242 (1987).
3. H. C. Fritts, *Tree Rings and Climate* (Academic Press, London, 1976).
4. W. Tranquillini, *Ecol. Stud.* **31**, 1–137 (1979).
5. K. R. Briffa *et al.*, *Nature* **346**, 434 (1990); K. R. Briffa *et al.*, *Clim. Dyn.* **7**, 111 (1992).
6. E. R. Cook, in *Methods of Dendrochronology*, E. R. Cook and L. A. Kairiukstis, Eds. (Kluwer Academic, Dordrecht, 1990), pp. 98–104.
7. D. A. Graybill, in *Climate from Tree Rings*, M. K. Hughes *et al.*, Eds. (Cambridge Univ. Press, Cambridge, 1982), pp. 21–30.
8. L. A. Scuderi, thesis, University of California, Los Angeles (1984).
9. The 38 series of ring widths that make up the chronology between A.D. 1 and 1981 range in length from 133 to 1183 years. The mean is 535 years; 70% of the series exceed 300 years in length, and 55% exceed 500 years. Chronology depth is 28 at A.D. 1800 and 19 at A.D. 1600. Depth varies from 9 to 19 between A.D. 1022 and 1600 with a minimum depth of 10 between A.D. 1 and 1021. Mean interseries correlation, a measure of the strength of the common signal in the chronology, is 0.397.
10. H. C. Fritts, T. Blasing, B. Hayden, J. Kutzbach, *J. Appl. Meteorol.* **10**, 845 (1971); K. Briffa and E. R. Cook, in (*6*), pp. 240–247; F. Serre-Bachet and L. Tessier, in *ibid.*, pp. 247–258.
11. S. W. Running and J. C. Coughlan, *Ecol. Modelling* **42**, 125 (1988).
12. G. C. Jacoby and R. D'Arrigo, *Clim. Change* **14**, 39 (1989).
13. V. C. LaMarche, Jr., *Science* **183**, 1043 (1974).
14. H. C. Fritts, J. Guiot, G. A. Gordon, in (*6*), pp. 178–185; G. A. Gordon and S. K. LeDuc, in *Seventh Conference on Probability and Statistics in Atmospheric Science* (Session 8, American Meteorological Society, Boston, 1981), pp. 129–133.
15. H. C. Fritts, *Reconstructing Large-Scale Climatic Patterns from Tree-Ring Data* (Univ. of Arizona Press, Tucson, AZ, 1991).
16. C. U. Hammer, H. B. Clausen, W. Dansgaard, *Nature* **288**, 230 (1980); R. B. Stothers, *ibid.* **307**, 344 (1984).
17. L. G. Drew, *Tree-Ring Chronologies of Western America: II. California and Nevada* (Chronology Series 1, Laboratory of Tree-Ring Research, Univ. of Arizona, Tucson, AZ, 1972).
18. H. C. Fritts and J. M. Lough, *Clim. Change* **7**, 203 (1985).
19. P. E. Damon and J. L. Jirikowic, in *Rare Nuclear Processes: Proceedings of the 14th Europhysics Conference on Nuclear Physics*, Bratislava, Czechoslovakia, 22 to 26 October 1990, P. Povinec, Ed. (World Scientific, Rivers Edge, NJ, 1992), pp. 177–201.
20. ———, in *Radiocarbon After Four Decades: An Interdisciplinary Perspective*, R. E. Taylor, A. Long, R. S. Kra, Eds. (Springer-Verlag, New York, 1992), pp. 117–129.
21. C. P. Sonett and S. A. Finney, *Philos. Trans. R. Soc. London* **330**, 413 (1990).
22. J. A. Eddy, *Clim. Change* **1**, 173 (1977).
23. M. Stuiver, T. F. Braziunas, B. Becker, B. Kromer, *Quat. Res. (NY)* **35**, 1 (1991).
24. C. P. Sonett and H. E. Suess, *Nature* **307**, 141 (1984).
25. M. Stuiver and T. F. Braziunas, *ibid.* **338**, 405 (1989).
26. ———, in *Secular Solar and Geomagnetic Variations in the Last 10,000 Years*, F. R. Stephenson and A. W. Wolfendale, Eds. (Kluwer, Dordrecht, the Netherlands, 1988), pp. 245–266.
27. M. R. Attolini, M. Galli, T. Nanni, *ibid.*, pp. 49–68.
28. J. Feynman and S. B. Gabriel, *Sol. Phys.* **127**, 393 (1990).
29. F. Rothlisberger, *10000 Jahre Gletschergeschichte der Erde* (Sauerländer, Aarau, Switzerland, 1986).

30. I thank R. Kerr, J. Drake, and two anonymous reviewers for comments that improved the content and clarity of this manuscript. Additional thanks to the Mount Whitney Ranger District, Lone Pine, CA, for continued access to sample sites, and to Boston University, which provided support for this study.

28 September 1992; accepted 15 December 1992

Export of North American Ozone Pollution to the North Atlantic Ocean

David D. Parrish,* John S. Holloway,† Michael Trainer, Paul C. Murphy,† Gerry L. Forbes, Fred C. Fehsenfeld†

Measurement of the levels of ozone and carbon monoxide (a tracer of anthropogenic pollution) at three surface sites on the Atlantic coast of Canada allow the estimation of the amount of ozone photochemically produced from anthropogenic precursors over North America and transported to the lower troposphere over the temperate North Atlantic Ocean. This amount is greater than that injected from the stratosphere, the primary natural source of ozone. This conclusion supports the contention that ozone derived from anthropogenic pollution has a hemisphere-wide effect at northern temperate latitudes.

Transport of pollutants from populated and industrialized continental areas affects the chemistry and radiation balance of the global atmosphere (*1*). A pollutant of particular interest is ozone (O_3), because its photolysis initiates the oxidizing processes in the atmosphere (*2*, *3*). Thus, the transport of O_3 from source regions affects the oxidizing capacity of the troposphere in the receptor areas. Additionally, O_3 is an important greenhouse gas whose atmospheric trends are only poorly known (*4*). Tropospheric O_3 has both natural and anthropogenic sources. The primary natural source is injection from the stratosphere (*5*, *6*). The anthropogenic source is photochemical production from precursors emitted by industrial and transportation combustion sources (*7*). To understand the budget, and hence the effects of O_3, it is important to quantify and to compare the magnitude of these two sources.

The heavily polluted eastern coast of